

# Preparation of TiO<sub>2</sub> Nanoelectrode and Its Application for Photoelectrochemical Catalytic Degradation of Malachite Green

Jianlian Liu<sup>1,3</sup>, Chaojun Du<sup>1,3</sup>, Chong Guo<sup>3</sup>, Lingli Zou<sup>2,\*</sup>

<sup>1</sup> School of Railway Transportation, Hunan Technical College of Railway High-Speed, Hengyang, Hunan, 421002, China

<sup>2</sup> Student Affairs Department, Hengyang Normal University, Hengyang, Hunan, 421001, China

<sup>3</sup> School of Biological and Chemical Engineering, Nanyang Institute of Technology, Nanyang, Henan 473004, China

\*E-mail: [tianxtpstar2020@163.com](mailto:tianxtpstar2020@163.com)

Received: 3 February 2022 / Accepted: 25 March 2022 / Published: 7 May 2022

---

Dye wastewater is a kind of industrial organic wastewater with large chroma and complex composition, and biochemical treatment is difficult to conduct. The discharge of dye wastewater will cause serious harm to water environment and human health. Electro-photocatalytic technology has received extensive social attention in the degradation of pollutants. Compared with the traditional physical, chemical and biochemical methods, it has the advantages of high efficiency, simple operation, non-selective degradation of environmental pollutants, and simple process equipment. Electrochemical anodic oxidation is a better method for the preparation of nanotube arrays. The electrode structure is stable and firmly bonded with the substrate. Therefore, in this work, TiO<sub>2</sub> nanotube arrays with different tube lengths were prepared by electrochemical anodic oxidation, and the effects of NaSO<sub>4</sub> solution concentration, voltage, initial pH value and initial concentration on electro-photocatalytic degradation of malachite green were investigated.

---

**Keywords:** Photoelectric chemistry; TiO<sub>2</sub> nanotubes; Malachite green; Pollution degradation; Anodic oxidation; Electron-hole pairs

## 1. INTRODUCTION

At present, with the development of global industrialization, worldwide environmental pollution is a big challenge [1]. As one of the major environmental pollution sources in the world, printing and dyeing industrial wastewater is usually discharged into rivers, lakes and seas without effective treatment, resulting in serious harm to water environment and human health [2,3]. Dye in dyeing wastewater is one of the main environmental pollution sources, most of which are aromatic and polyheterocyclic compounds with colored groups (such as N=N-, -N=O) [4,5]. Since the dye wastewater has the

characteristics of high organic content, complex composition, and deep chroma and is difficult to biodegrade, it will reduce the transmittance of light and affect the growth of aquatic plants after being discharged to water [6,7]. In addition, wastewater can also hinder its self-purification in the water body. Some dyes accumulated in the environment can generate aromatic amine intermediates under the anaerobic action of microorganisms, bringing about potential environmental risks [8]. Therefore, the removal of dyes has become the primary problem to be solved in the treatment of printing and dyeing wastewater. At present, there are three commonly applied methods to treat dye wastewater, including physical method, chemical method and biological method [9]. Despite that these three methods are of great significance to the treatment of dye wastewater, all of these traditional methods have various defects. Physical treatment is costly and has a narrow application scope, and it is easy to produce a large number of refractory substances [10,11]. Chemical processes may produce toxic by-products and large amounts of sludge, and its operating cost is high. The biological treatment method is not good for chromaticity removal and the dye contaminants cannot be completely degraded. Therefore, to find a kind of efficient, clean dye processing technology with suitable range and low cost has become the current environmental protection goal [12].

Electrochemical oxidation method refers to the electron transfer reaction of organic matter or metal ions in the electrolytic cell on the electrode under the action of electric field [13]. These reactions can make toxic and harmful substances oxidized into non-toxic and harmless substances or become precipitation and gas separated from the solution, thus achieving the purpose of removing pollutants [14,15]. According to different mechanism of oxidation, it can be divided into direct oxidation on and near the anode surface and indirect oxidation away from the electrode surface. Electrochemical oxidation has mild reaction conditions and high energy utilization. The reaction requires less chemical agents, which is a safe, clean and efficient water treatment method [16–18]. However, due to the limitation of electrode materials, electrochemical oxidation degrades organic matter with low efficiency and high energy consumption, which limits its application in practice.

Photocatalytic oxidation method refers to the application of light irradiation on the n-type semiconductor photocatalyst surface (such as  $\text{TiO}_2$ ,  $\text{SnO}_2$ ,  $\text{ZnS}$ ,  $\text{WO}_3$ , etc.), which can prompt the electrons in the semiconductor valence band to be excited to transit to the conduction band [19,20]. Meanwhile, the corresponding holes are generated in the conduction band of the catalyst, thus forming photogenerated electrons and holes in the semiconductor. Photogenerated electrons have strong reducibility and the holes have strong oxidation.  $\cdot\text{OH}$  with strong oxidizing ability can be formed by the action of holes and adsorbed water on oxide surface [21].  $\cdot\text{OH}$  can combine, replace, and transfer electrons with organic pollutants to oxidize organic pollutants into simple inorganic substances. Photocatalytic oxidation has a bright advantage in the degradation of organic pollutants in water, especially those pollutants that are difficult to biodegrade [22,23]. However, it is still far away from industrial production for the reason that it cannot fully utilize solar energy and the processing equipment is complex [24–26].

In the research and application of photocatalysis, two obvious problems are presented: 1) The separation and recovery of catalyst powder is difficult [27]; 2) The photocatalytic efficiency is not high due to the high recombination probability of photogenerated electrons and holes. In order to solve these problems, researchers proposed the photoelectric catalytic oxidation technology. The catalyst is fixed on

a conductive substrate and also acts as a working electrode [28]. The photogenerated electrons are forced to move towards the opposite electrode by anodic voltage and separated from the photogenerated holes, thus improving the photocatalytic efficiency [29].

In this work, nanotube arrays were prepared by anodic oxidation with Ti sheets as substrates. The advantage of TiO<sub>2</sub> nanotube array is that it is easy to recycle and reuse. The prepared TiO<sub>2</sub> nanotubes were adopted for electro-photocatalytic degradation of malachite green solution. Different conditions were applied in exploring the best degradation conditions for industrial application.

## 2. EXPERIMENTAL

Hydrofluoric acid, perchloric acid, sodium fluoride, phosphoric acid, ammonium fluoride, malachite green and ethylene glycol were purchased with national pharmaceutical reagents. Ti pieces were purchased from Hengye Fengchan Materials Co., LTD.

Electrode pretreatment: the titanium foil with a thickness of 0.15 cm was cut into Ti sheets with a width of 15 cm and a width of 1.5 cm. After being ground and mechanically polished with 1#, 3# and 6# sandpaper, the surface became smooth. After ultrasonic oscillation cleaning, the Ti sheet was immersed in 0.1 M HClO<sub>4</sub> + 0.02 M NaF solution and chemically polished for 30 s. The cleaned Ti sheets were placed in the air to dry naturally.

Constant potential oxidation: constant potential oxidation was conducted with two electrode system. The working electrode and counter electrode were titanium and platinum, respectively. All experiments were carried out at room temperature. The electrolytic cell was filled with about 80 mL 0.15 M NH<sub>4</sub>F + 0.5 M H<sub>3</sub>PO<sub>4</sub>, V(water) : V(ethylene glycol) = 3:7 electrolyte. 20 V was adopted for electrochemical etching. The whole process of the experiment continued under magnetic agitation. After the electrochemical etching, the electrodes were removed and the surface was slowly washed with distilled water before the next step of heat treatment.

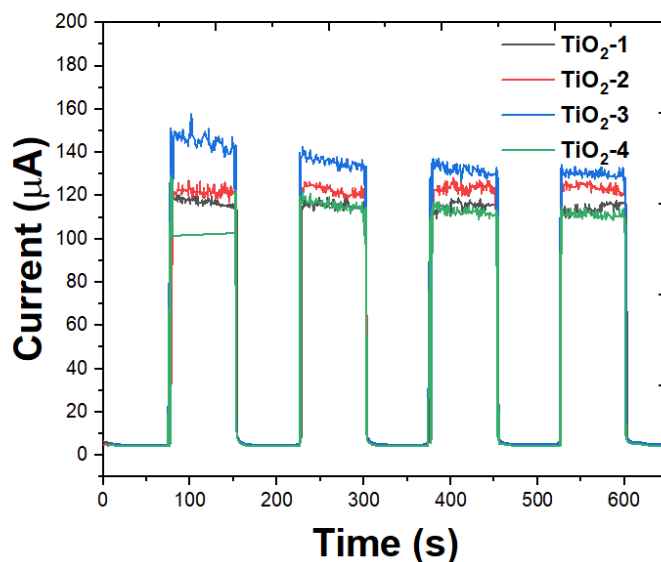
Heat treatment: the prepared Ti nanotubes in the above step was placed under a muffle furnace for high temperature calcination. The temperature was increased from room temperature to 500°C at a rate of 5 °C/min. After 3 h of constant calcination, TiO<sub>2</sub> nanotube electrodes were formed and cooled to room temperature naturally for further use. The TiO<sub>2</sub> nanotube electrodes prepared by 1, 2, 3 and 4 h electrochemical etching were denoted as TiO<sub>2</sub>-1, TiO<sub>2</sub>-2, TiO<sub>2</sub>-3 and TiO<sub>2</sub>-4.

The photochemical test was performed by CHI760E. The nanotube electrode, saturated calomel electrode and platinum electrode were applied as working electrode, reference electrode and contrast electrode respectively. In the photoelectric test experiment, xenon lamp of 500W was adopted as the simulated sunlight source.

## 3. RESULTS AND DISCUSSION

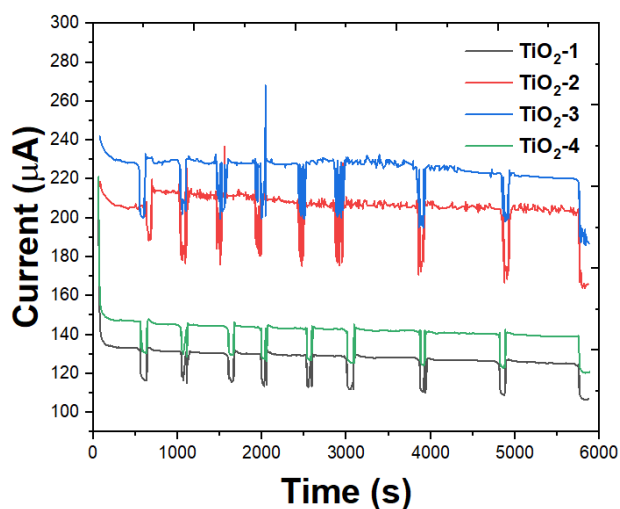
The change of current with time under constant potential was first studied in this work, which can reflect the change of current in electrochemical reaction and the electron transfer on the surface of

the nanotube electrode. Figure 1 shows I-T curves of photocurrent response of TiO<sub>2</sub> nanotubes in dark and bright state transients in 1 M NaOH solution. As can be seen from the figure, the current of each TiO<sub>2</sub> nanotube electrode in the dark state is almost 150  $\mu$ A, and after the application of voltage and light, the electrode samples all produce obvious photocurrent response, indicating that the prepared nanotube has good photoresponse performance.



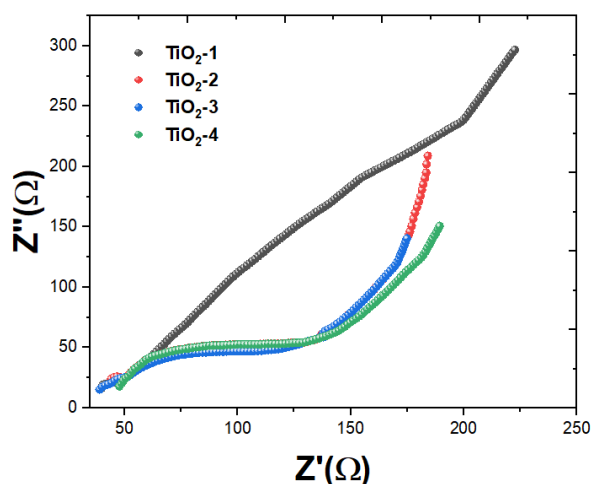
**Figure 1.** Full illumination I-T curves of TiO<sub>2</sub>-1, TiO<sub>2</sub>-2, TiO<sub>2</sub>-3 and TiO<sub>2</sub>-4 in 1 M NaOH solution with light-on and light-off.

Figure 2 shows the I-T curves of different nanotubes illuminated in malachite green. It can be seen that TiO<sub>2</sub>-3 presented the strongest current model, the reason for which may be that electrodes with different morphologies have different photophysical carrier generation abilities [30,31].



**Figure 2.** Full illumination I-T curve of malachite green degradation by different TiO<sub>2</sub>-1, TiO<sub>2</sub>-2, TiO<sub>2</sub>-3 and TiO<sub>2</sub>-4 during the light-on and light-off cycles in 0.01M Na<sub>2</sub>SO<sub>4</sub>.

Electrochemical impedance spectroscopy (EIS) is a common electrochemical analysis method, which has a wide measurement range and has been adopted for the study of electrode surface phenomena [32,33]. In addition, EIS can obtain more information about the dynamic parameters and interface structure of the electrode performance, thus revealing the relationship between the transport characteristics of photogenerated carriers and the electro-photocatalytic activity of semiconductor materials [34]. Figure 3 shows the EIS curves of malachite green degradation with different nanotube electrodes under full illumination. It can be noted from the figure that the radius of capacitive arc is  $TiO_2-1 > TiO_2-4 > TiO_2-2 > TiO_2-3$ . According to the principle of EIS spectrum, the radius is positively correlated with the resistance, which means that the radius is negatively correlated with the photocurrent, thus the photocurrent corresponding to each nanotube electrode is  $TiO_2-3 > TiO_2-2 > TiO_2-4 > TiO_2-1$ .



**Figure 3.** EIS curves of  $TiO_2-1$ ,  $TiO_2-2$ ,  $TiO_2-3$  and  $TiO_2-4$  in malachite green solution (0.01M  $Na_2SO_4$ ).

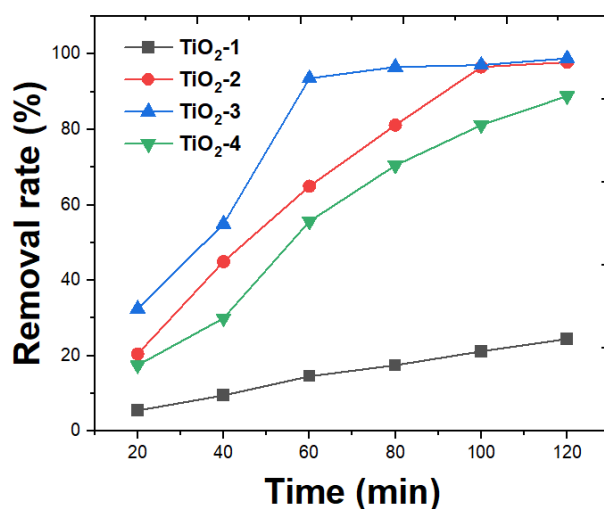


**Figure 4.** Removal rate of  $TiO_2-1$ ,  $TiO_2-2$ ,  $TiO_2-3$  and  $TiO_2-4$  on degradation of malachite green (0.01M  $Na_2SO_4$ ).

The initial concentration of malachite green degradation is 15 mg/L. The concentration of  $\text{Na}_2\text{SO}_4$  is 0.01 M. Figure 4 shows the effect of four different nanotube electrodes on the degradation of malachite green. The figure presents that the removal rate of malachite green is only 14.6% after  $\text{TiO}_2$ -1 for 60 min.

The removal rate of malachite green with  $\text{TiO}_2$ -2 is about 65.0%, while the removal rate of malachite green is up to 93.6% after the electro-photocatalytic activity of  $\text{TiO}_2$ -3 for 60 min. However, the removal rate of malachite green decreases to 55.7% after the electro-electro-photocatalytic activity of  $\text{TiO}_2$ -4 for 60 min. The possible reasons for the excellent performance of  $\text{TiO}_2$  nanotube electrode are as follows :1) photogenerated electrons and hole pairs are generated in the photocatalyst under the condition of light, and the applied voltage is conducive to the transfer of photogenerated electrons in the electro-photocatalytic process to the opposite electrode [35,36]. This process reduces the recombination probability of photogenerated electron-hole pairs produced by  $\text{TiO}_2$  and increases the amount of  $\cdot\text{OH}$  produced in the electro-photocatalytic process [37]. 2) The chemical capture of photogenic electrons generated by the electrolytic water side reaction generates  $\text{O}_2^-$ . It can not only be directly used for oxidative degradation of malachite green, but also further react to produce  $\cdot\text{OH}$  [38].

In the electro-photocatalytic process, electrolyte concentration mainly affects the degradation of malachite green by affecting the conductivity of the solution, hence it is necessary to choose the concentration of electrolyte solution reasonably [39]. Anhydrous  $\text{Na}_2\text{SO}_4$  was selected as electrolyte in this experiment in order to exclude the active species with strong oxidation ability formed by chloride ion plasma in the electro-photocatalytic process, thus interfering with the experimental results of electro-photocatalytic experiment [40]. Under the condition that the initial concentration of malachite green is 15 mg/L, the  $\text{TiO}_2$ -3 is used as the working electrode, and the voltage is 10V. Table 1 compares this material with several similar electrodes adopted for malachite green degradation.

**Table 1.** Electrochemical degradation of malachite green using different electrode materials.

Electrode materials	Degradation (min)	time	Malachite green concentration (mg/L)	Degradation efficiency (%)	Reference
FTO	20	10		97.67	[41]
$\text{PbO}_2$	90	15		99.6	[42]
$\text{TiO}_2$ -3	60	15		93.6	This work

The influence of  $\text{Na}_2\text{SO}_4$  solution with different concentrations on the electro-photocatalytic degradation of malachite green was investigated in this study. As shown in Figure 5, the degradation rate of malachite green increases with  $\text{Na}_2\text{SO}_4$  concentration from 0.005 M to 0.03 M. When the concentration of  $\text{Na}_2\text{SO}_4$  is 0.03 M, the degradation rate reaches the maximum. The degradation rate of malachite green begin to decrease with the increase of electrolyte concentration. This trend may be resulted from the following two aspects: firstly, it can be explained by the mechanism of electrolyte diffusion and migration. Increasing the concentration of electrolyte essentially increases the conductivity of solution [43,44]. When  $\text{Na}_2\text{SO}_4$  concentration is low, the ionic concentration of the solution is very low, which makes the current leading to the solution small and electrochemical reactions less likely to

occur. As the concentration of  $\text{Na}_2\text{SO}_4$  increases, the concentration of ions in the solution increases, and so does the current [45], which is beneficial to the promotion of electrochemical direct oxidation and the production of active substances, thus increasing the degradation rate of malachite green. When the electrolyte concentration increases to a certain degree, the bypass current in the reaction system increases if the electrolyte concentration continues to increase. In the meantime, the side reaction of electrolysis is intensified, and the adsorption competition between  $\text{Na}_2\text{SO}_4$  and malachite green on the electrode surface increases [46]. Malachite green is less adsorbed to the electrode surface. In addition, excessive current results in dissolution of the active component from the particle electrode. Therefore, the increasing concentration of  $\text{Na}_2\text{SO}_4$  decreases the treatment effect. Secondly, despite that the addition of electrolyte can increase the conductivity of the solution, the electrochemical oxidation efficiency increases. However, many researchers believe that  $\text{SO}_4^{2-}$  can capture  $\text{H}^+$  or  $\cdot\text{OH}$  to produce  $\text{SO}_4^{\cdot-}$  under light. The weak oxidation of  $\text{SO}_4^{\cdot-}$  is not sufficient to degrade malachite green. As a result, excessive  $\text{SO}_4^{2-}$  can inhibit malachite green degradation. In a certain concentration range, the concentration of  $\text{SO}_4^{\cdot-}$  increases with the concentration of  $\text{SO}_4^{2-}$  in the solution. Therefore, when the concentration of  $\text{Na}_2\text{SO}_4$  gradually increases, the electro-photocatalytic degradation can first rise to a certain degree, and then begin to decrease.

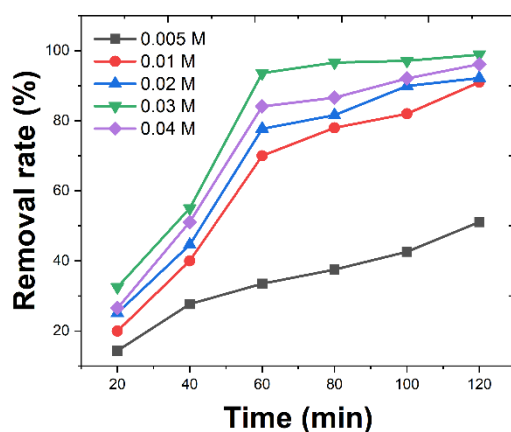


**Figure 5.** Effect of  $\text{Na}_2\text{SO}_4$  concentration on electro-photocatalytic degradation of malachite green (0.01M  $\text{Na}_2\text{SO}_4$ ) using  $\text{TiO}_2$ -3.

Applied voltage is an important factor affecting wastewater treatment with electrochemical oxidation technology. It is the original driving force for electrochemical oxidation reactions. Most theories hold that electrochemical oxidation degradation of organic compounds includes direct electrochemical oxidation and indirect electrochemical oxidation. In the direct electrochemical oxidation process, when the voltage is greater than the redox potential of the reactant, the redox reaction of gaining and losing electrons takes place. Generally, the higher the voltage is, the more it is conducive to the electrolytic reaction [47–50]. In the indirect electrochemical oxidation process,  $\cdot\text{OH}$ ,  $\text{H}_2\text{O}_2$ ,  $\text{O}_3$  and  $\text{Cl}_2/\text{ClO}^-$  are strongly oxidizing active substances. Through the reaction of these active substances and

organic matter in water, the organic matter is completely oxidized into small molecular organic matter or inorganic matter [51–54].

The applied voltage can not only provide driving force for direct electrolysis of organic pollutants, but also promote the separation of photoelectron-hole pairs generated by the photocatalyst on the surface of the electrode during the illumination reaction. Hence the applied voltage is a key factor affecting the electro-photocatalytic degradation rate. Therefore, in this study, the effect of applying different applied voltages on the photoelectric degradation of malachite green was investigated, and the results are shown in Figure 6. It can be found from the figure that when the applied voltage increases from 4 V to 8 V, the photoelectric degradation rate of malachite green increases with the voltage. The possible reason for this phenomenon is that the effective working electrode area increases with the voltage[55–57]. The direct and indirect electrochemical oxidation of organic pollutants on the electrode surface can be enhanced. Increasing the voltage is also beneficial to the promotion of the separation of photoelectron-hole pair and the improvement of the reaction rate of electro-photocatalytic malachite green. However, when the voltage exceeds 8 V and continues to rise, the photoelectric degradation rate of malachite green continues to increase but begins to decrease, the reason for which may be that the number of photoelectron-hole pairs is fixed as the light intensity is fixed. When the voltage increases to a certain value, the photogenerated electrons and holes are sufficiently separated to form a saturated photocurrent. At this time, increasing the voltage will not increase the degradation rate, but will aggravate the side reaction of anodic oxygen evolution and cathodic ammonia evolution [58]. A large number of bubbles produced affect the adsorption of malachite green on the electrode surface, and inhibit the reaction rate of photoelectricity degradation of rhodamine.

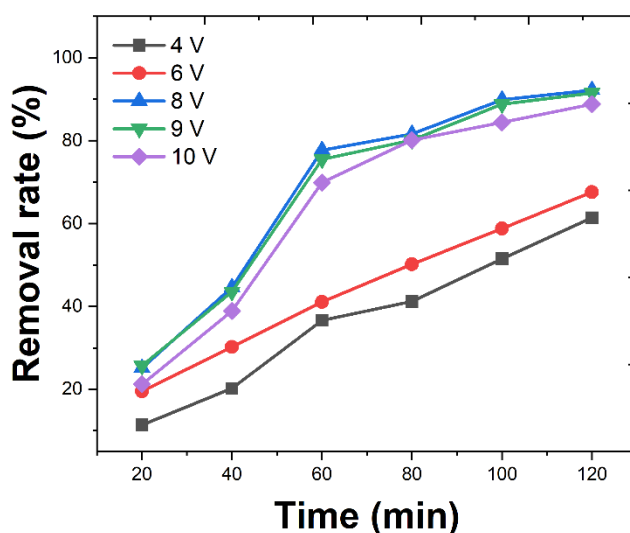


**Figure 6.** Effect of applied voltage on electro-photocatalytic degradation of malachite green (0.01M  $\text{Na}_2\text{SO}_4$ ) using  $\text{TiO}_2$ -3.

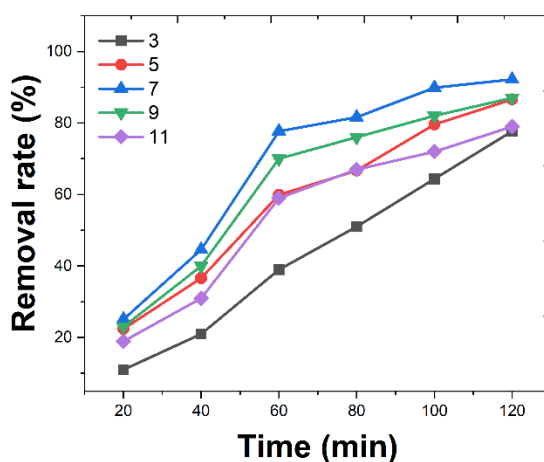


**Figure 7.** Effect of initial pH on electro-photocatalytic degradation of malachite green (0.01M Na<sub>2</sub>SO<sub>4</sub>) using TiO<sub>2</sub>-3.

pH value is also a key factor in electro-photocatalytic degradation of organic matter, and the influence of electro-photocatalytic reaction is a very complex process. It is generally believed that in the electro-photocatalytic process, the influence of pH value is mainly manifested in the following two aspects: on the one hand, pH value affects the charge on the TiO<sub>2</sub> surface and the ionic morphology of organic compounds, thus affecting the adsorption and desorption capacity of organic compounds on the electrode surface [59–61]. On the other hand, pH value can affect the migration of photocarriers and the formation of active groups in the photocatalytic reaction. Figure 7 illustrates the effect of different pH values on photoelectrochemical degradation of malachite green.

As shown in Figure 7, under acidic conditions (pH = 3–7), the photoelectric degradation rate of malachite green decreases with the increase of pH value from 3 to 7. Under alkaline condition (pH = 7–11), the photoelectric degradation rate of malachite green accelerates with the increase of pH value. The possible reason for this fact is that pH value affects the form of malachite green, and further affects the adsorption of malachite green on the electrode surface [62]. On the other hand, pH value affects the formation of active substances in the system.

Figure 8 shows the effect of different initial concentrations on electro-photocatalytic degradation of malachite green. According to the figure, when the initial concentration of malachite green is 15 mg/L, the degradation rate reaches the maximum, and the removal rate reaches 92.2% after 60 min. Excessively low or high concentration will reduce the removal rate. The reasons for this phenomenon may be as follows: firstly, there are certain active sites on the electrode surface, and the degradation reaction generally occurs at these active sites. Under the condition of low initial concentration of malachite green, the active site can not completely be bound to malachite green. The electro-photocatalytic degradation efficiency of malachite green is low due to the residual active sites. With the increase of malachite green concentration, the adsorption of malachite green on the active site reaches saturation at a certain value, and the degradation rate is the maximum at this time. When the concentration of malachite green continues to increase, malachite green accumulates on the electrode surface, resulting in the reduction of the active site. Therefore, increasing the concentration will not increase the degradation rate.

Secondly, with the increase of malachite green concentration, the light transmittance of malachite green solution decreases, and the light energy reaching the electrode surface decreases. The reduction of photoelectron-hole pair yield is not conducive to the formation of surface active substances, such as free radicals, thus reducing the electro-photocatalytic degradation rate.

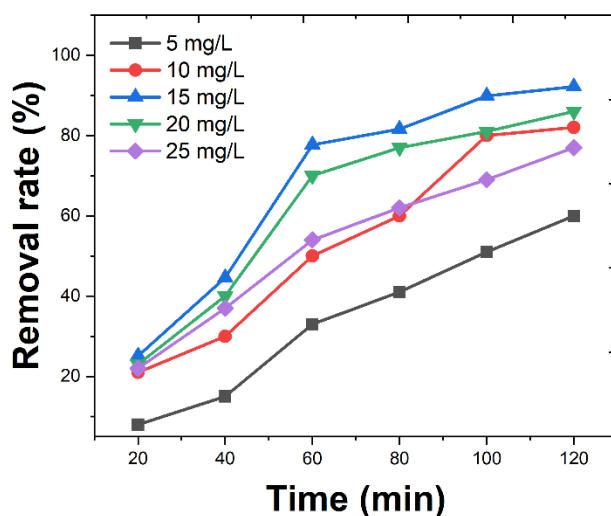


**Figure 8.** Effect of initial concentration on electro-photocatalytic degradation of malachite green (0.01M Na<sub>2</sub>SO<sub>4</sub>) using TiO<sub>2</sub>-3.

#### 4. CONCLUSION

TiO<sub>2</sub> nanotube electrode was prepared by electrochemical anodic oxidation in this work. According to the photocurrent response and EIS of TiO<sub>2</sub> nanotubes in the light-dark transient process, it can be concluded that TiO<sub>2</sub> nanotubes deposited for 3 h have better photoelectric response performance. Afterwards, the electro-photocatalytic degradation of malachite green was carried out with TiO<sub>2</sub> nanotubes deposited for 3 h. Electrolyte concentration mainly affects the degradation effect of malachite green through the change of the solution conductivity. The experimental results indicate that when malachite green is in the process of electro-photocatalytic degradation, there is an optimal value of electrolyte concentration, excessively high or low electrolyte concentration will weaken the photocatalytic effect to a certain extent. In the electro-photocatalytic reaction system, the applied voltage is mainly the driving force of electrode polarization and the photoelectron-hole pair separation. The electro-photocatalytic degradation of malachite green can be improved by increasing the applied voltage of electrolytic cell. However, overly high voltage will aggravate the side reaction and accelerate the oxidation of electrode, thus affecting the degradation effect. The degradation rate of malachite green is higher in acidic condition and alkaline condition, but the degradation rate of malachite green in acidic condition is higher than that in alkaline condition, the reason for which is that on the one hand, pH value affects the form of malachite green, thus affecting the adsorption of malachite green on the electrode surface, while on the other hand, pH value affects the formation of active substances in the system.

## ACKNOWLEDGMENTS

This work was supported by (1) the Education Department of Henan Province (Project #20B530004); (2) Nanyang Science and Technology Bureau (Project #JCQY004); and (3) Nanyang Key Laboratory of Catalytic Functional Materials; (4) Interdisciplinary Sciences Project, Nanyang Institute of Technology

## References

1. S. Zhao, H. Zhu, Z. Wang, P. Song, M. Ban, X. Song, *Chemical Engineering Journal*, 353 (2018) 460.
2. B. Yuan, C. Zhang, Y. Liang, L. Yang, H. Yang, L. Bai, D. Wei, W. Wang, Q. Wang, H. Chen, *Advanced Sustainable Systems*, 5 (2021) 2000245.
3. N.Y. Donkadokula, A.K. Kola, I. Naz, D. Saroj, *Reviews in Environmental Science and Bio/Technology*, 19 (2020) 543.
4. H. Chen, Y.J. Zhang, P.Y. He, C.J. Li, H. Li, *Applied Surface Science*, 515 (2020) 146024.
5. Y. Zhao, W. Yu, R. Li, Y. Xu, Y. Liu, T. Sun, L. Shen, H. Lin, *Applied Surface Science*, 483 (2019) 1006.
6. D. Guo, Y. Xiao, T. Li, Q. Zhou, L. Shen, R. Li, Y. Xu, H. Lin, *Journal of Colloid and Interface Science*, 560 (2020) 273.
7. A.S. Reddy, S. Kalla, Z.V.P. Murthy, *Journal of Water Process Engineering*, 46 (2022) 102610.
8. Y. Kang, J. Jang, S. Kim, J. Lim, Y. Lee, I.S. Kim, *ACS Appl. Mater. Interfaces*, 12 (2020) 36148.
9. J.K.H. Wong, H.K. Tan, S.Y. Lau, P.-S. Yap, M.K. Danquah, *Journal of Environmental Chemical Engineering*, 7 (2019) 103261.
10. M. Jiang, K. Ye, J. Deng, J. Lin, W. Ye, S. Zhao, B. Van der Bruggen, *Environ. Sci. Technol.*, 52 (2018) 10698.
11. M. Ajaz, A. Rehman, Z. Khan, M.A. Nisar, S. Hussain, *AMB Express*, 9 (2019) 64.
12. T. My Hanh Le, R. Nuisin, R. Mongkolnavin, P. Painmanakul, S. Sairiam, *Separation and Purification Technology*, 288 (2022) 120711.
13. D. Liu, J. Yin, H. Tang, H. Wang, S. Liu, T. Huang, S. Fang, K. Zhu, Z. Xie, *Separation and Purification Technology*, 279 (2021) 119755.
14. H. Zhao, R. Wang, H. Deng, L. Zhang, L. Gao, L. Zhang, T. Jiao, *ACS Omega*, 6 (2021) 294.
15. W. Li, B. Mu, Y. Yang, *Bioresource Technology*, 277 (2019) 157.
16. K. Rambabu, G. Bharath, F. Banat, P.L. Show, *Journal of Hazardous Materials*, 402 (2021) 123560.
17. F. Mashkoo, A. Nasar, *Journal of Magnetism and Magnetic Materials*, 500 (2020) 166408.
18. N. Jaafarzadeh, A. Takdastan, S. Jorfi, F. Ghanbari, M. Ahmadi, G. Barzegar, *Journal of Molecular Liquids*, 256 (2018) 462.
19. Y.-M. Chu, Q.-V. Bach, *Applied Nanoscience* 7 (2020) 55.
20. S. Adhikari, D.-H. Kim, *Applied Surface Science*, 511 (2020) 145595.
21. H.D. Bouras, Z. Isik, E. Bezirhan Arikian, N. Bouras, A. Chergui, H.C. Yatmaz, N. Dizge, *Biochemical Engineering Journal*, 146 (2019) 150.
22. S. Rajagopal, B. Paramasivam, K. Muniyasamy, *Separation and Purification Technology*, 252 (2020) 117444.
23. N. Li, G. Chen, J. Zhao, B. Yan, Z. Cheng, L. Meng, V. Chen, *Journal of Membrane Science*, 591 (2019) 117341.
24. G. Başaran Dindaş, Y. Çalışkan, E.E. Çelebi, M. Tekbaş, N. Bektaş, H.C. Yatmaz, *Journal of Environmental Chemical Engineering*, 8 (2020) 103777.
25. L. Liu, Z. Chen, J. Zhang, D. Shan, Y. Wu, L. Bai, B. Wang, *Journal of Water Process Engineering*, 42 (2021) 102122.
26. G. Pan, X. Jing, X. Ding, Y. Shen, S. Xu, W. Miao, *Journal of Alloys and Compounds*, 809 (2019) 151749.

27. S.R. Yousefi, H.A. Alshamsi, O. Amiri, M. Salavati-Niasari, *Journal of Molecular Liquids*, 337 (2021) 116405.
28. A. Singh, S. Kumar, B. Ahmed, R.K. Singh, A.K. Ojha, *Journal of Alloys and Compounds*, 806 (2019) 1368.
29. M.S. Kumar, S.H. Sonawane, B.A. Bhanvase, B. Bethi, *Journal of Water Process Engineering*, 23 (2018) 250.
30. L. Lin, W. Jiang, M. Bechelany, M. Nasr, J. Jarvis, T. Schaub, R.R. Sapkota, P. Miele, H. Wang, P. Xu, *Chemosphere*, 220 (2019) 921.
31. H. Qiu, R. Zhang, Y. Yu, R. Shen, H. Gao, *Science of The Total Environment*, 706 (2020) 136043.
32. R. Ata, G. Yildiz Töre, *Journal of Environmental Management*, 233 (2019) 673.
33. A. Talaiekhosani, M. Reza Mosayebi, M.A. Fulazzaky, Z. Eskandari, R. Sanayee, *Alexandria Engineering Journal*, 59 (2020) 549.
34. S. Dong, L. Cui, W. Zhang, L. Xia, S. Zhou, C.K. Russell, M. Fan, J. Feng, J. Sun, *Chemical Engineering Journal*, 384 (2020) 123279.
35. S. Wang, Z. Wu, J. Chen, J. Ma, J. Ying, S. Cui, S. Yu, Y. Hu, J. Zhao, Y. Jia, *Ceramics International*, 45 (2019) 11703.
36. N. Bahadur, N. Bhargava, *Journal of Water Process Engineering*, 32 (2019) 100934.
37. W.-N. Du, S.-T. Chen, *Journal of Environmental Management*, 206 (2018) 507.
38. M.R. Al-Mamun, S. Kader, M.S. Islam, M.Z.H. Khan, *Journal of Environmental Chemical Engineering*, 7 (2019) 103248.
39. D. Chen, Y. Cheng, N. Zhou, P. Chen, Y. Wang, K. Li, S. Huo, P. Cheng, P. Peng, R. Zhang, L. Wang, H. Liu, Y. Liu, R. Ruan, *Journal of Cleaner Production*, 268 (2020) 121725.
40. Y. Wang, X. Sun, T. Xian, G. Liu, H. Yang, *Optical Materials*, 113 (2021) 110853.
41. Y. Chen, D. Fan, L. Huang, Y. Li, Z. Qiu, C. Feng, *Int. J. Electrochem. Sci*, 15 (2020) 11437–11453.
42. Y. Diao, F. Wei, L. Zhang, Q. Zhao, H. Sun, Y. Yao, *Null*, 102 (2022) 1126.
43. S. Zhang, B. Li, X. Wang, G. Zhao, B. Hu, Z. Lu, T. Wen, J. Chen, X. Wang, *Chemical Engineering Journal*, 390 (2020) 124642.
44. S. Marimuthu, A.J. Antonisamy, S. Malayandi, K. Rajendran, P.-C. Tsai, A. Pugazhendhi, V.K. Ponnusamy, *Journal of Photochemistry and Photobiology B: Biology*, 205 (2020) 111823.
45. J. Ai, L. Hu, Z. Zhou, L. Cheng, W. Liu, K. Su, R. Zhang, Z. Chen, W. Li, *Ceramics International*, 46 (2020) 11786.
46. W.A.A. Mohamed, I.A. Ibrahim, A.M. El-Sayed, H.R. Galal, H. Handal, H.A. Mousa, A.A. Labib, *Advanced Powder Technology*, 31 (2020) 2555.
47. A. Ansari, D. Nematollahi, *Applied Catalysis B: Environmental*, 261 (2020) 118226.
48. M. Chen, H. Yang, Z. Song, Y. Gu, Y. Zheng, J. Zhu, A. Wang, L. Fu, *Phyton-International of Experimental Botany*, 90 (2021) 1507.
49. D. Wang, D. Li, L. Fu, Y. Zheng, Y. Gu, F. Chen, S. Zhao, *Sensors*, 21 (2021) 8216.
50. H. Karimi-Maleh, Y. Orooji, F. Karimi, M. Alizadeh, M. Baghayeri, J. Rouhi, S. Tajik, H. Beitollahi, S. Agarwal, V.K. Gupta, *Biosensors and Bioelectronics* (2021) 113252.
51. H. Jiang, A. Xue, Z. Wang, R. Xia, L. Wang, Y. Tang, P. Wan, Y. Chen, *Sustainable Chemistry*, 1 (2020) 345.
52. B. Fan, Q. Wang, W. Wu, Q. Zhou, D. Li, Z. Xu, L. Fu, J. Zhu, H. Karimi-Maleh, C.-T. Lin, *Biosensors*, 11 (2021) 155.
53. Y. Zheng, D. Wang, X. Li, Z. Wang, Q. Zhou, L. Fu, Y. Yin, D. Creech, *Biosensors*, 11 (2021) 403.
54. L. Fu, S. Mao, F. Chen, S. Zhao, W. Su, G. Lai, A. Yu, C.-T. Lin, *Chemosphere*, 297 (2022) 134127.
55. H. Karimi-Maleh, A. Khataee, F. Karimi, M. Baghayeri, L. Fu, J. Rouhi, C. Karaman, O. Karaman, R. Boukherroub, *Chemosphere* (2021) 132928.

56. H. Karimi-Maleh, C. Karaman, O. Karaman, F. Karimi, Y. Vasseghian, L. Fu, M. Baghayeri, J. Rouhi, P. Senthil Kumar, P.-L. Show, S. Rajendran, A.L. Sanati, A. Mirabi, *Journal of Nanostructure in Chemistry* (2022) in-press.
57. M.R. Samarghandi, A. Dargahi, A. Shabanloo, H.Z. Nasab, Y. Vaziri, A. Ansari, *Arabian Journal of Chemistry*, 13 (2020) 6847.
58. Y. Wang, M. Chen, C. Wang, X. Meng, W. Zhang, Z. Chen, J. Crittenden, *Chemical Engineering Journal*, 374 (2019) 626.
59. Y. Xia, Q. Dai, *Chemosphere*, 205 (2018) 215.
60. Y. Yao, M. Li, Y. Yang, L. Cui, L. Guo, *Chemosphere*, 216 (2019) 812.
61. C. Zhou, Y. Wang, J. Chen, L. Xu, H. Huang, J. Niu, *Chemosphere*, 225 (2019) 304.
62. F. Zhang, W. Wang, L. Xu, C. Zhou, Y. Sun, J. Niu, *Chemosphere*, 278 (2021) 130465.

© 2022 The Authors. Published by ESG ([www.electrochemsci.org](http://www.electrochemsci.org)). This article is an open access article distributed under the terms and conditions of the Creative Commons Attribution license (<http://creativecommons.org/licenses/by/4.0/>).